International Journal of Multidisciplinary Research and Modern Education (IJMRME)
ISSN (Online): 2454 - 6119
(www.rdmodernresearch.org) Volume I, Issue I, 2015

WIRELESS AND WEARABLE EEG SYSTEM FOR PREVENTING THE VEHICLE ACCIDENT

A. K. Nivedha*, A. Dinesh Kumar, Mohammed Aslam***, Muhammed Nadeer*** & Shithin. B. S*****

* Assistant Professor, Department of Biomedical Engineering, Dhanalakshmi Srinivasan Engineering College, Perambalur, Tamil Nadu
** Assistant Professor, Department of Mathematics, Dhanalakshmi Srinivasan Engineering College, Perambalur, Tamil Nadu
*** UG Scholar, Department of Biomedical Engineering, Dhanalakshmi Srinivasan Engineering College, Perambalur, Tamil Nadu

Abstract:

A real time wireless Electroencephalogram (EEG) sensor system for drowsiness detection. Drowsy driving has been implicated as a casual factor in many accidents. Therefore real time drowsiness monitoring can prevent traffic accidents effectively. In this study, EEG sensor system was developed to monitor the human cognitive state and provide biofeedback to the driver when the drowsy state occurs. The proposed system consist a driver status in order to link the fluctuation of driver performance with changes in brain activity and process the EEG recordings. This detection system allows for earlier detection of driver drowsiness than driving pattern detection, But it is limited accuracy and insufficient reaction time in current driver drowsiness detection system have lead to the exploration of new techniques based on changes in body physiology as a function of fatigue. One promising method is the use of signals recorded from scalp electrodes that measure pattern of changing electrical activity in the brain as someone goes from a state of complete alertness to fatigue and drowsiness. This work performed a sustained-attention driving task and warning feedback system might lead to a practical closed-loop system to predict, monitor and rectify

Keywords: EEG Sensor & Drowsiness Detection

1. Introduction:

Long-term, monotonous, or nighttime driving often lowers driving performance. As is widely assumed, drowsiness significantly contributes to automobile accidents, leading to a considerable number of traffic collisions, injuries, and fatalities annually. Developing an effective system for detecting drowsiness is thus of priority concern for real-life driving. Such an in-vehicle system must continuously monitor the arousal status of drivers and accurately predict the potential Several bio-behavioral signatures have been developed to monitor drowsiness of automobile drivers, including eye blinking and head nodding. However, false alarms are Likely since these visual attributes are not always accompanied by drowsiness. Related studies in recent decades have demonstrated that electroencephalography (EEG), i.e., the electric fields produced by brain activity, is a highly effective Physiological indicator for assessing vigilance states. EEG is the only brain imaging modality with a high temporal and fine spatial resolution that is sufficiently lightweight to be worn in operational settings. Numerous EEG studies suggest that delta (1–3 Hz), theta (4–7 Hz), and alpha (8–12Hz) activities are highly correlated with fatigue, drowsiness, Based on the neurological findings, drowsiness monitoring algorithms were developed by using several machine learning methods. The experimental results further demonstrated the feasibility of detecting or monitoring driver drowsiness level using EEG signals. However, designing a user acceptable and feasible EEG device to realize the real-time monitoring system is still a challenging task. Data collection in most EEG studies requires skin preparation and

conductive gel application to ensure excellent electrical conductivity between a sensor and human skin. These procedures are time consuming, uncomfortable, and even painful for participants. Additionally, the signal quality may degrade over time as the conductive gel dries out. Hence, a wearable and wireless dry-electrode EEG system must be developed, capable of assessing the brain activities of participants performing ordinary tasks. According to a previous study, spectral dynamics of EEG at posterior brain regions are strongly correlated with the deterioration of task performance and declining vigilance.

In the power spectra were successfully linked with behavioral performance by regression models. Additionally, the advantage of using the EEG signals of the posterior brain region has been shown in a recent study that the classification performance of the drowsiness detection system using the EEG signals of parietal and occipital regions is significantly better than that using the EEG signals of the frontal region. However, these studies still used conventional wet EEG electrodes in measuring EEG signals. Hence, acquiring the EEG signal of the hair region is a critical factor in developing a successful vigilance monitoring system. Recent studies have measured EEG signals using dry sensors, including silicone conductive rubber, comb-like electrode, gold-plated electrode, bristle-type electrode, and foam-based sensor. Table I lists some commercially available EEG systems. Most of these dry sensors are useful for hairy sites. EEG acquisition from the posterior region is available; this study develops an EEG-based in-vehicle system for assessing human vigilance level. EEG dynamics and behavioral changes of participants are simultaneously recorded via a new dry-contact EEG device with spring-loaded sensors when they perform a sustained-attention driving task.
Additionally, an effective system using support vector regression (SVR) is developed to model the relationship between the brain activity and the behavioral performance. The system performance of SVR-based model is compared with other state-of-art regression methods. Moreover, the prediction model is implemented on a portable device. Furthermore, feasibility of the proposed system is demonstrated by monitoring human cognitive states during a sustained-attention driving task.

2. System Architecture:

Fig. 1 shows the proposed EEG-based in-vehicle system, designed to monitor human vigilance level continuously during automobile driving. To construct the system, EEG signals were recorded using a mobile and wireless EEG device with dry sensors in a realistic dynamic driving simulator [32]. For data acquisition, the wireless and mobile EEG system, as shown in Fig. 2,consists of dry electrodes, data acquisition module, Bluetooth transition module, and rechargeable battery. The device was designed for quickly and conveniently recording an EEG signal of the occipital region which is highly correlated with the vigilance. This dry EEG system surpasses the conventional wet electrodes with the conduction gel for long-term EEG measurements. Additionally, the signal quality of the used dry EEG system is comparable with that of the NeuroScan. For data analysis, the pre-stimulus EEG spectra of all experimental trials were segmented and formed as a training dataset of samples after applying band-pass filter (0.5–50 Hz) and fast Fourier transformation (FFT) [33]. Each training sample was accompanied with the behavioral performance in response to the given task, indicating the presumable vigilance of a driver. As for the core of the prediction system, the relationship between EEG and behavior was modelled using support vector regression (SVR). Finally, the predicted outputs were converted to different levels of vigilance. For real-world applications, the proposed system was implemented on a mobile device using JAVA programming language. The wireless and wearable EEG device transmitted its recorded

data via a Bluetooth interface to the user's device. The acquired EEG is displayed, processed, and analyzed in real time. The following sections introduce in detail the major components of the proposed system.

Dry EEG Electrodes: As shown in Fig. 2(a)–(c), a new dry-contact EEG device with spring-loaded sensors was proposed for potential operations in the presence or absence of hair and without any skin maintaining the Integrity of the Specifications preparation or conductive gel usage. Each probe was designed to include a probe head, plunger, spring, and barrel. The 17 probes were inserted into a flexible substrate using a one-time forming process via an established injection molding procedure. With 17 spring contact probes, the flexible substrate allows for a high geometrical conformity between the sensor and the irregular scalp surface to maintain low skin-sensor interface impedance. Additionally, the flexible substrate also initiates a sensor buffer effect, Thereby eliminating pain when force is applied. This sensor is more convenient than conventional wet electrodes in measuring EEG signals without any skin preparation or conductive gel usage. The flexible substrate also initiates a sensor buffer effect, and not as an independent document. Please do not revise any of the current designations. Brain sense is a sleek, single-channel, wireless headset that monitors your brain activity and translates EEG in to meaningful data you can understand. The biosensor platform provides a powerful for the development of a variety of application that promotes mind health such improved focus, concentration, working memory and acuity. Other uses include meditation and relaxation monitoring or improved educational processes. Our low cost, complete OEM solution is a high-performance bio-signal on a single chip solution for accurate mind activity detection and processing. Brain sense uses neurosky. TGAM-1 module, its high performance Bluetooth module hc-05. This is a standalone BTM-05 Bluetooth module, its work as TTL master/slave transceiver module with serial part protocol for communication. Designed by full speed Bluetooth operation with full piconet support it allows you to achieve the industry's highest levels of sensitivity, accuracy, with lowest power consumption

EEG Signal Acquisition Circuit: According to Fig. 2(d), the EEG acquisition module consists of four major components [28]: a amplifier (ISL28470,Intersil, USA);, a front-end analog-to-digital converter (ADC, AD1298, Analog Devices, USA), a microcontroller (MSP430, Texas Instruments, USA), and a wireless transmission (BM0403, Unigrand Ltd., Taiwan). The voltage between the electrode and the reference was amplified using a biosignal amplifier with high input impedance. Meanwhile, the common-mode noise was rejected to precisely detect microvolt-level brain wave signals from the scalp. In particular, transfer function of the preamplifier, i.e., equivalent to the form of a high-pass filter with input signals of frequency, is as follows: The amplified signal was digitized via an ADC with a 24 bit Resolution and 256 Hz sampling rate. The minimum input voltage of ADC ranges from to 1.94 mV. The maximum input voltage of ADC ranges from to 23.30 mV. In the microcontroller unit, the power-line interface was removed using a moving average filter with a frequency of 60 Hz. The digitalized signals after amplification and filtering were transmitted to a PC or a mobile device via Bluetooth with a baud-rate of 921600 bits/s. Power was supplied by a high capacity (750 mAh, 3.0 V) Li-ion battery, which provided 23 hr of continuous operation at maximum power consumption.

EEG Signal Processing and Analysis: During a 90 min driving experiment (see Section III), the study participants encountered hundreds of unexpected lane-departure events. In the signal processing, all 2 s baseline data (512 sampling points) before the stimuli were extracted from continuous EEG signals. The data in this baseline period, without

any confounding factors (i.e., events, motion stimuli, and motor actions) were an appropriate segmentation of EEG signals to link the physiological message with the driving performance. The data pair of the *t*-th trial is denoted as number of trial and refers to the driving performance, as measured by the reaction time (RT) in response to the lane-departure event. First, a type I Chebyshev band-pass filter with cut-off frequencies of 0.5 Hz and 50 Hz was applied on the raw data to remove artifacts. Second, physiological features were extracted by transforming the EEG signals of all trials, In to a frequency domain using FFT to characterize the spectral dynamics of brain activities. As shown in Fig. 4, the EEG signal was successively fed into a weighted time-frequency analysis before applying support vector regression. Power spectral density (PSD) of the EEG signal at time

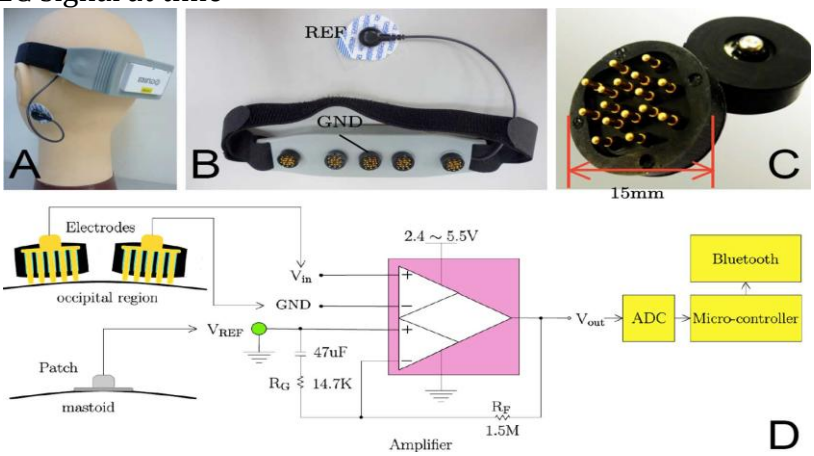

Fig (1) Wireless and wearable EEG devices (a) Wireless and wearable EEG headsets (b) Five dry EEG electrodes and one patch sensor (c) Spring-loaded probes (d) Block diagram of the circuit

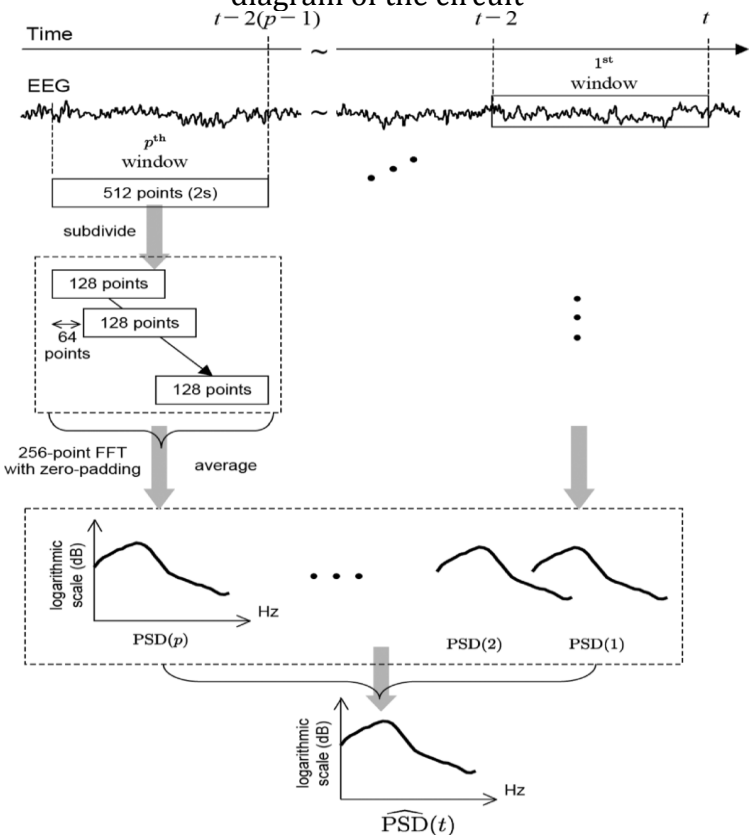

Fig (2): Spectral EEG feature extraction

Power spectra at time, denoted by are estimated by using FFT with Welch's method and a weighting scheme, where the spectral feature are extracted every 2 s. windows of EEG spectrum, in which all frequency responses of EEG activations were calculated using a 512-point moving window without overlapping points. Each 512 points (2 s) of data were further subdivided into several 128-point sub-windows advanced in a 64-point step. Windowed 128-point epochs were extended to 256 points by zero-padding in order to calculate the power spectra using a 256-point FFT (Welch's method), subsequently yielding an estimate of the power spectral density with 30 frequency bins from 1 to 30 Hz. The power spectra of these sub-windows were converted into a logarithmic scale and averaged to form a log power spectrum for each window. Furthermore, the estimated spectral powers of four channels were averaged, and the mean power spectrum of the first 10 min of the experiment, which was putatively the alert pattern, was subtracted from each estimated spectrum. Since the periods of the cyclic fluctuations of drowsiness exceeded 4 min, variance at cycle lengths shorter than 1 Min was eliminated using a weighted-averaging filter that advanced in a step of 2 s. Next, PSD of the window was multiplied by a weighted coefficient, where w decreased as Increased. In this study, and. compared with an unprocessed PSD without a weighted-averaging

Prediction Model: According to previous studies, the behavioral lapses induced by drowsiness correlate with the changes of EEG activities. To link the power spectra with RTs, a nonlinear model is preferred in the model fitting to cover linear and nonlinear relationships between EEG power spectra and RTs. The support vector machine is a conventional means of solving the multidimensional function estimation problem, and has been applied to various fields such as classification and regression. When used to solve the function approximation and regression estimation problems, SVM is denoted as the support vector regression (SVR). Fig. 2 shows the graphical framework of SVR, including the support vectors, mapped vectors, and dot product operations. SVR is a complex and heavy-computational implementation of a forecasting algorithm based on structuring risk minimization principles to obtain an effective generalization capability SVR, can be formulated as minimization of and the following: where determines the width of RBF function, is a constant trading off the higher-order versus lower-order term in the polynomial, is a scaling parameter of the input data, and is a shifting parameter controlling the threshold of mapping. The root mean square error (RMSE) is a conventional index for evaluating the performance of the predictor [40]. RMSE can be estimated as follows:

3. Experimental Design and Materials:

Subjects: Fifteen subjects participated in a sustained-attention driving task. Each subject wore a wireless and wearable EEG headset, sat inside the vehicle, and controlled the simulator by using the steering wheel. To easily induce drowsiness, the experiment began in the early afternoon (13:00–14:00) after lunch and lasted for approximately 90 min when the circadian rhythm of sleepiness reached its peak.

Driving Simulator: As shown in Fig. 3(a), the synchronized scenes were projected from six projectors to constitute a surrounding 360 vision. At the center of the projected scenes, a real vehicle (without the unnecessary weight of an engine and other components) was mounted on a six degree-of-freedom motion platform. The motion sensation was then delivered along with the movement of the vehicle. A four-lane highway scene projected on a surrounding screen simulates a visually monotonous and unexciting stimulus of a driving condition to induce drowsiness. Additionally, the refresh rate of the highway scene was set properly to emulate a car driving at a fixed

speed of 100 km/hr. The four lanes from left to right were separated by a median strip. The distance from the left side to the right side of the road was equally divided into 240 units (digitized into values of 1–240): the widths of each lane and the car were 60 units and 28 units, respectively. This unit was converted.

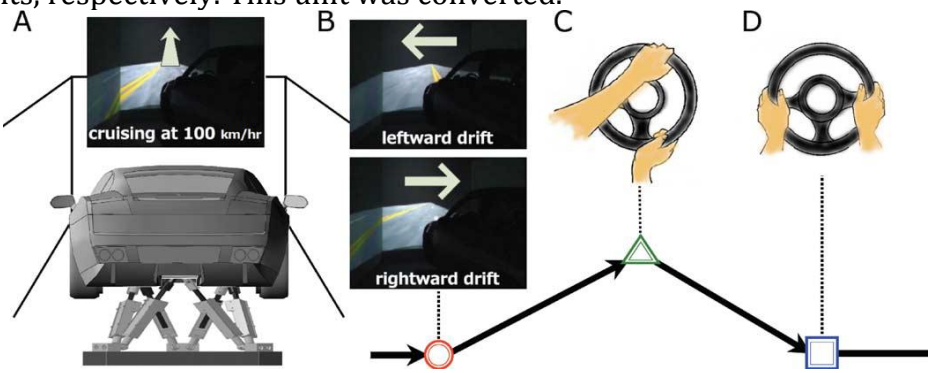

Fig (3) Sustained-attention driving task implemented in an immersive driving simulator (a) the driving simulator was mounted on a motion platform. The VR scene simulates nighttime cruising at a speed of 100 km/hr on a four-lane highway without other traffic (b) The event-related lane-departure paradigm Deviation onset: the time interval when the car starts to drift to the right or left of the cruising lane (c) Response onset: the time interval when subjects use the steering wheel. (d) Response offset: the time interval when the car returns to the original lane into the same ratio of the width of the real lane (3.75 m) and the car (1.8 m). Additionally, the server also received the data via RS-232 compatible serial port from the client which ran the VR programand recorded the behavioral response. This data stream with an 8-bit digital resolution including the vehicle trajectory (0–240), deviation onset (251/252 for left and right side of the deviation), response onset (253), and response offset (254), was synchronized with the EEG data for further event-related analysis.

Experimental Paradigm: The event-related land-departure paradigm (Fig. 3) was implemented in the VR driving simulator. This paradigm attempted to replicate a non ideal road surface to make the car randomly drift out of the cruising lane (deviation onset) at a deviation speed of 5 km/hr toward the left or right side. When encountering each lane-departure event [Fig. 3(b)], which occurred approximately every 8–12 s, the subject was instructed to steer the car (response onset) back to the center of the original lane (response offset) immediately [Fig. 3(c)]. During a 90 min experiment, the total number of trials available from each subject was next, the subject's vigilance level in each trial was quantified using the reaction time (RT, the duration between the deviation onset and the response onset). As is assumed, although the subject was alert during the experiment, their RT was fast, whereas a slow RT accompanied the occurrence of drowsiness.

4. Experimental Results:

Relationship between RTS and Power Spectra: Fig (4) shows the spectral EEG changes in response to changes in the increase of RT, where denotes the square of Pearson's correlation coefficient. The power spectra of four EEG recordings were averaged and converted into a logarithmic scale in order to form a log power spectrum. Amplitudes of the 2 s prestimulus EEG spectrum were then used to correlate with the following RT. Most studies identified significant increases in the delta and theta activities, which were strongly leads to confusion because equations do not balance dimensionally. If you must use mixed units, clearly state the units for each quantity that you use in an equation.

System Performance: The feasibility of predicting drivers' vigilance level based on spectral EEG patterns was examined by comparing the prediction performance of using the power spectra of 1–30 Hz as the feature vectors for training a SVR. The prediction performances of SVR using linear, polynomial, radial basis function (RBF), and sigmoid kernel functions were also compared. Regarding the performance validation (Table II), two-fold cross-validation was performed and run 100 times to yield the average results. Restated, half of data (257 samples) were randomly selected as the training data, and the remaining data (257 samples) were selected as the validation data. The performance was evaluated by the root mean square error (RMSE) and squared between the recorded RT and the predicted RT. The number of trained support vectors was also reported. Each cell represents the of the measures. In terms to using the EEG features, SVR with a RBF kernel trained by the alpha power yields the lowest RMSE and the highest, compared to the delta (RMS), theta (RMSE:), and beta powers (RMSE: When using the concatenation of four band powers, RMSE decreased to and the increased to .Moreover, the RMSE decreases to and the increased to when RBF-SVR used the spectral power of 1–30 Hz as the feature vectors.

The number of support vectors tended to decrease if the number of features increased. Additionally, SVR with a RBF kernel, which was trained by the spectral power of 1–30 Hz, used the least number of support vectors (36% of the data), compared to other methods (50–70% of the data). The highlighted cells indicate the optimum results among all of the combinations of learning algorithms and spectral features. Overall, SVR using a RBF kernel yields higher prediction accuracy than that using linear, polynomial, and sigmoid kernel functions. According to the safety distance between vehicles reported by the Road Safety Authority [49], a minimum reaction distance of 20 m is recommended when driving at a speed of 100 km/h. Notably, the RMSEs obtained by the proposed system ranges from 124 ms to 481 ms (about 3–13 m at a 100 km/hr car speed), which does not violate the recommended reaction distance. Additionally, the best performance of this study is comparable with our previous result (RMSE: 130 ms) [13] in which the drowsiness detection system used the EEG signals acquired by the NeuroScan. Fig. 4 further compares the prediction result of SVR using different kernel functions, where SVR was trained by using the spectral powers of 1–30 Hz. The black trace is the recorded RT sorted from fast to slow, and the color traces are RT predicted by different methods. The black bars denote the absolute differences between the recorded RT and the predicted RT. This finding clearly indicates that SVR with a RBF kernel had a higher prediction accuracy than that of other methods, especially for the prediction of fast and slow RTs. Additionally, the uniform distribution of prediction errors across the entire spectrum of RT revealed how the RBF-based SVR provided the desired robustness for forecasting human behaviors. In our previous study [50], polymer foam-based sensors were used in the dry EEG system to record subject's forehead EEG signal. Although RMSE of the prediction result was comparable

Fig (4): RTs predicted by support vector regression using (a) linear (b) polynomial (c) RBF, and (d) sigmoid kernels. Black and color traces indicate the recorded RT and the prediction RT, respectively. Black bars denote the prediction errors (i.e., absolute difference between recorded RTs and predicted RTs). With those obtained in this study

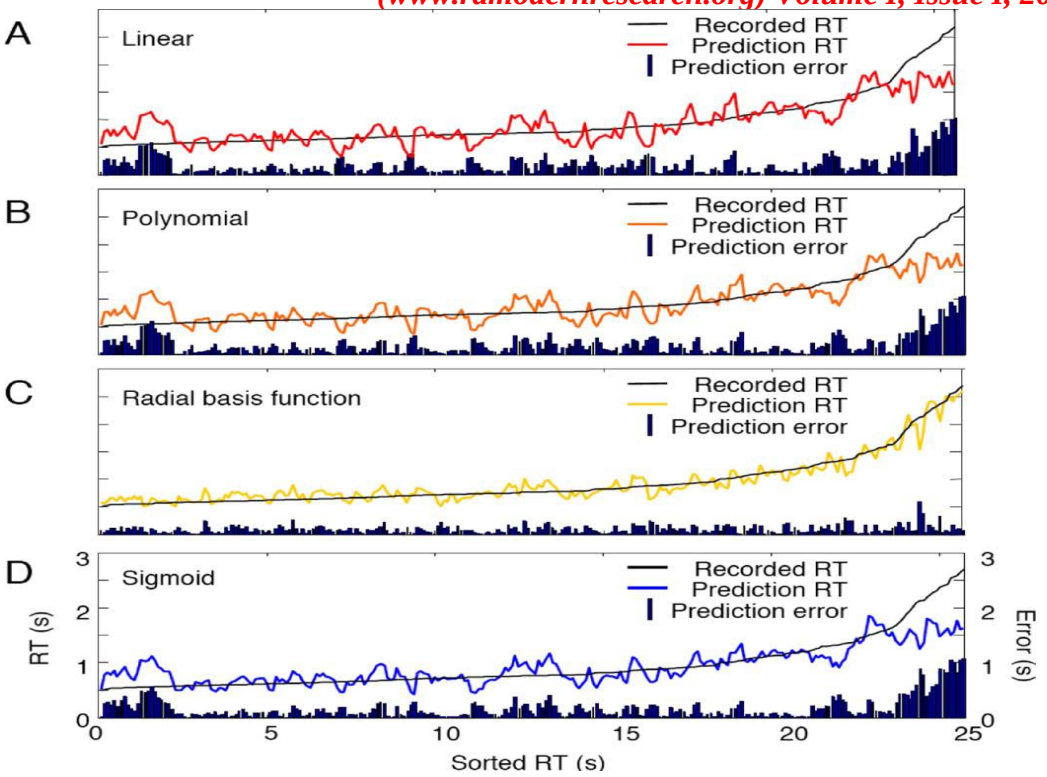

Real-Time Vigilance Prediction: Above results suggest that the EEG-based system using the RBF-based SVR is a highly promising means of predicting the driver's vigilance level. An attempt was also made to verify the feasibility of the proposed system by further implementing the SVR model in Java language as an Android application, in which the parameters of the implemented model (including slack parameter of SVR, gamma value of RBF kernel, and support vectors of the obtained model) were trained using Mat lab software. Fig. 9 shows a temporal relationship between the vigilance levels predicted by the proposed system and driver's behavior in response to regular traffic events or emergencies when the participant performed the lane-departure driving task for approximately 70 min. The predicted results were converted into eight degrees of vigilance level every 2 s according to Table III which shows the conversion of predicted RT into vigilance level. At the beginning of the experiment, the relatively alert state (bluish bars was predicted and lasted continuously for several minutes)

5. Conclusion:

This study developed a driver vigilance prediction system with a wireless and wearable EEG device, an efficient prediction model, and a real-time mobile App to remedy for drowsy driving. Based on the proposed EEG system, a link was established between the fluctuation in the behavioral index of driving performance (i.e., increase in RT) and the changes in the brain activity (i.e., trends in EEG power spectra). Experimental results indicated that the RMSE could minimize to 0.124 ms when the SVR with a RBF kernel was applied as the prediction model. Additionally, this SVR-based prediction model was implemented in real time for the subjects.

6. References:

1. F. Vaca, J. S. Harris, H. G. Garrison, and M. P. McKay, "Drowsy driving," Ann. Emerg. Med., vol. 45, no. 4, pp. 433–434, 2005.
2. P. P. Caffier, U. Erdmann, and P. Ullsperger, "Experimental evaluation of eye-blink parameters as a drowsiness measure," Eur. J. Appl. Physiol., vol. 89, no. 3, pp. 319–325, 2003.

3. Q. Ji, Z. Zhu, and P. Lan, "Real-time nonintrusive monitoring and prediction of driver fatigue," IEEE Trans. Veh. Technol., vol. 53, no. 4, pp. 1052–1068, Jul. 2004.
4. J. Horne and L.Reyner, "Vehicle accidents related to sleep: A review," Occupat. Environ. Med., vol. 56, no. 5, pp. 289–294, May 1999.
5. S. K. L. Lal and A. Craig, "A critical review of the psychophysiology of driver fatigue," Biol. Psychol., vol. 55, no. 3, pp. 173–194, Feb. 2001.
6. S. Makeig and T.-P. Jung, "Tonic, phasic, and transient EEG correlates of auditory awareness in drowsiness," Cogn. Brain Res., vol. 4, no. 1, pp. 15–25, 1996.
7. S. K. L. Lal and A. Craig, "Driver fatigue: Electroencephalography and psychological assessment," Psychophysiol., vol. 39, no. 3, pp. 313–321, 2002.
8. L. Chin-Teng, C. Che-Jui, L. Bor-Shyh, H. Shao-Hang, C. Chih-Feng, and I. J. Wang, "A real-time wireless brain-computer interface system for drowsiness detection," IEEE Trans. Biomed. Circuits Syst., vol. 4, no. 4, pp. 214–222, Aug. 2010.
9. C. Guger et al., "How many people are able to control a P300-based brain-computer interface (BCI)," Neurosci. Lett., vol. 462, no. 1, pp. 94–98, Oct. 2009.
10. M. A. Schier, "Changes in EEG alpha power during simulated driving: A demonstration," Internat. J. Psychophysiol., vol. 37, no. 2, pp. 155–162, Aug. 2000.
11. C. Papadelis et al., "Monitoring sleepiness with on-board electrophysiological recordings for preventing sleep-deprived traffic accidents," Clin. Neurophysiol., vol. 118, no. 9, pp. 1906–1922, Sep. 2007.
12. S. Makeig, T.-P. Jung, and T. Sejnowski, "Awareness during drowsiness: Dynamics and electrophysiological correlates," Can. J. Exp. Psychol., vol. 54, no. 4, pp. 266–273, 2000.
13. F.-C. Lin, L.-W. Ko, C.-H. Chuang, T.-P. Su, and C.-T. Lin, "Generalized EEG-based drowsiness prediction system by using a self-organizing neural fuzzy system," IEEE Trans. Circuits Syst. I, Reg. Papers, vol. 59, no. 9, pp. 2044–2055, Sep. 2012.
14. C.-T. Lin et al., "Tonic and phasic EEG and behavioral changes induced by arousing feedback," NeuroImage, vol. 52, no. 2, pp. 633–642, Aug. 2010.
15. C.-T. Lin, C.-H.Chuang, Y.-K.Wang,S.-F. Tsai,T.-C. Chiu, andL.-W. Ko, "Neurocognitive characteristics of the driver: A review on drowsiness, distraction, navigation, and motion sickness," J. Neurosci. Neuroengin., vol. 1, no. 1, pp. 61–81, Jun. 2012.
16. C.-T. Lin, I.-F. Chung, L.-W. Ko, Y.-C. Chen, S.-F. Liang, and J.-R. Duann, "EEG-based assessment of driver cognitive responses in a dynamic virtual-reality driving environment," IEEE Trans. Biomed. Eng., vol. 54, no. 7, pp. 1349–1352, Jul. 2007.
17. C. H. Chuang, L. W. Ko, Y. P. Lin, T. P. Jung, and C. T. Lin, "Independent component ensemble of EEG for brain-computer interface," IEEE Trans. Neural Syst. Rehabil. Eng., vol. 22, no. 2, pp. 230–238, Mar. 2014.
18. T. C. Ferree, P. Luu, G. S. Russell, and D.M. Tucker, "Scalp electrode impedance, infection risk, and EEG data quality," Clin. Neurophysiol., vol. 112, no. 3, pp. 536–544, Mar. 2001.
19. X. Jiawei, R. F. Yazicioglu, B. Grundlehner, P. Harpe, K. A. Makinwa, and C. Van Hoof, "A 160 muW 8-channel active electrode system for EEG monitoring," IEEE Trans. Biomed. Circuits Syst., vol. 5, no. 6, pp. 555–567, Dec. 2011.
20. T. I. Oh et al., "Nanofiber web textile dry electrodes for long-term biopotential recording," IEEE Trans. Biomed. Circuits Syst., vol. 7, no. 2, pp. 204–11, Apr. 2013.
21. G. Gargiulo et al., "A new EEG recording system for passive dry electrodes," Clin. Neurophysiol., vol. 121, no. 5, pp. 686–693, May 2010.
22. T. O. Zander et al., "A dry EEG-system for scientific research and brain-computer interfaces," Front Neurosci., vol. 5, no. 53, pp. 1–10, 2011.

23. Brainwave EEG Signal, NeuroSky, Dec. 5, 2009 [Online]. Available: http://www.neurosky.com
24. C. Grozea, C. D. Voinescu, and S. Fazli, "Bristle-sensors—low-cost flexible passive dry EEG electrodes for neurofeedback and BCI applications," J. Neural. Eng., vol. 8, no. 2, pp. 1–8, Apr. 2011.
25. C.-T. Lin, L.-D. Liao, Y.-H. Liu, I.-J. Wang, B.-S. Lin, and J.-Y. Chang, "Novel dry polymer foam electrodes for long-term EEG measurement," IEEE Trans. Biomed. Eng., vol. 58, no. 5, pp. 1200–1207, 2011.
26. L.-D. Liao et al., "Biosensor technologies for augmented brain-computer interfaces in the next decades," Proc. IEEE, vol. 100, pp. 1553–1566, May 2012, Special Centennial Issue.
27. L.-D. Liao et al., "Gaming control using a wearable and wireless EEG based brain-computer interface device with novel dry foam-based sensors," J. Neuroeng. Rehabil., vol. 9, no. 5, pp. 1–11, Jan. 2012.
28. L.-D. Liao, I.-J. Wang, S.-F. Chen, J.-Y. Chang, and C.-T. Lin, "Design, fabrication and experimental validation of a novel dry-contact sensor for measuring electroencephalography signals without skin preparation," Sensors, vol. 11, no. 6, pp. 5819–5834, 2011.
29. L. D. Liao et al., "A novel 16-channel wireless system for electroencephalography measurements with dry spring-loaded sensors," IEEE Trans. Instrum. Meas., vol. 63, no. 6, pp. 1545–1555, Jun. 2014.
30. R.-S. Huang, T.-P. Jung, and S.Makeig, "Tonic changes in EEG power spectra during simulated driving," Lecture Notes Comput. Sci., vol. 5638 LNAI, pp. 394–403, 2009.
31. C.-T. Lin, I. F. Chung, L.-W. Ko, Y.-C. Chen, S.-F. Liang, and J.-R. Duann, "EEG-based assessment of driver cognitive responses in a dynamic virtual-reality driving environment," IEEE Trans. Biomed. Eng., vol. 54, no. 7, pp. 1349–1352, Jul. 2007.
32. W. Karlen, C. Mattiussi, and D. Floreano, "Sleep and wake classification with ECG and respiratory effort signals," IEEE Trans. Biomed. Circuits Syst., vol. 3, no. 2, pp. 71–78, Apr. 2009.
33. M. A. Haberman and E. M. Spinelli, "A multichannel EEG acquisition scheme based on single ended amplifiers and digital DRL," IEEE Trans. Biomed. Circuits Syst., vol. 6, no. 6, pp. 614–618, Dec. 2012.
34. D. Neamen, Microelectronics Circuit Analysis and Design, 3rd ed. New York, NY, USA: McGraw-Hill, 2007.
35. S. Makeig and M. Inlow, "Lapses in alertness: Coherence of fluctuations in performance and EEG spectrum," Electroencephalogr. Clin. Neurophysiol., vol. 86, no. 1, pp. 23–35, Jan. 1993.
36. U. Thissen, M. Pepers, B. Üstün, W. J. Melssen, and L.M. C. Buydens, "Comparing support vectormachines to PLS for spectral regression applications," Chemometr. Intell. Lab. Syst., vol. 73, no. 2, pp. 169–179, 2004.
37. C.-C. Chang and C.-J. Lin, "LIBSVM: A Library for support vector machines," ACM
38. L. Sheiner and S. Beal, "Some suggestions for measuring predictive performance," J. Pharmacok. Biopharm., vol. 9, no. 4, pp. 503–512, 1981.
39. H. J. Moller, L. Kayumov, E. L. Bulmash, J. Nhan, and C. M. Shapiro, "Simulator performance, microsleep episodes, and subjective sleepiness: Normative data using convergent methodologies to assess driver drowsiness," J. Psychosom. Res., vol. 61, no. 3, pp. 335–42, Sep. 2006.
40. M. Ferrara and L. D. Gennaro, "How much sleep do we need?," Sleep Med. Rev., vol. 5, no. 2, pp. 155–179, Apr. 2001.

41. R. S. Huang, T. P. Jung, and S. Makeig, "Tonic changes in EEG power spectra during simulated driving," Lecture Notes Comput. Sci., vol. 5638 LNAI, pp. 394–403, Dec. 2009.
42. S. Banks, P. Catcheside, L. Lack, R. R. Grunstein, and R. D. McEvoy, "Low levels of alcohol impair driving simulator performance and reduce perception of crash risk in partially sleep deprived subjects," Sleep, vol. 27, no. 6, pp. 1063–1067, Sep. 2004.
43. B. T. Jap, S. Lal, P. Fischer, and E. Bekiaris, "Using EEG spectral components to assess algorithms for detecting fatigue," Expert Syst. Applicat., vol. 36, no. 2, pp. 2352–2359, Mar. 2009.
44. H. J. Eoh, M. K. Chung, and S.-H. Kim, "Electroencephalographic study of drowsiness in simulated driving with sleep deprivation," Int. J. Ind. Ergonom., vol. 35, no. 4, pp. 307–320, 2005.